Hosting various guests including fullerenes and free radicals in versatile organic paramagnetic bTbk open frameworks

Bardelang, David; Giorgi, Michel; Hornebecq, Virginie; Stepanov, Anatoli; Hardy, Micael; Rizzato, Egon; Monnier, Valerie; Zaman, Md. Badruz; Chan, Gordon; Udachin, Konstantin; Enright, Gary; Tordo, Paul; Ouari, Olivier

Publisher's version / Version de l'éditeur:
https://doi.org/10.1021/cg401097e
Crystal Growth and Design, 14, 2, pp. 467-476, 2014-12-10

CRYSTAL GROWTH & DESIGN

Article

pubs.acs.org/crystal

Hosting Various Guests Including Fullerenes and Free Radicals in Versatile Organic Paramagnetic bTbk Open Frameworks

David Bardelang,*[,†] Michel Giorgi,[‡] Virginie Hornebecq,[§] Anatoli Stepanov,[∥] Micaël Hardy,[†] Egon Rizzato,[†] Valérie Monnier,[‡] Md. Badruz Zaman,[⊥,▽] Gordon Chan,[#] Konstantin Udachin,[#] Gary Enright,[#] Paul Tordo,[†] and Olivier Ouari*[,†]

[†]Aix-Marseille Université, CNRS UMR7273, Institut de Chimie Radicalaire (ICR), case 521, Avenue Escadrille Normandie-Niemen, 13397 Marseille, Cedex 20, France

[‡]Aix-Marseille Université, Spectropole, FR 1739 - Fédération des Sciences Chimiques de Marseille, Faculté des Sciences de Saint-Jérôme, Case A62, Avenue Escadrille Normandie Niemen, 13397 Marseille, Cedex 20, France

[§]Aix-Marseille Université et CNRS, Equipe S2P, Laboratoire MADIREL, UMR 7246, Centre de Saint-Jérôme, F-13397 Marseille, Cedex 20, France

[∥]Aix-Marseille Université et CNRS, IM2NP, UMR 6242, Faculté des Sciences et Techniques de Saint-Jérôme, Avenue Escadrille Normandie-Niemen, 13397 Marseille, Cedex 20, France

[⊥]Center of Excellence for Research in Engineering Materials, Faculty of Engineering, King Saud University, Riyadh 11421, Saudi Arabia

[#]National Research Council of Canada, 1200 Montreal Road, Ottawa, Ontario K1A0R6 Canada

Supporting Information

ABSTRACT: The dinitroxide bis(TEMPO) bisketal (**bTbk**) was shown to crystallize into open frameworks whose structures were determined by single-crystal X-ray diffraction. We show that **bTbk** can be used as a supramolecular building block for the hosting of a plethora of guests inside the 1D channels of its paramagnetic framework, including other radicals such as TEMPO or 2-azaadamantane-*N*-oxyl. C_{60} and C_{70} were also found to be easily included in this open framework during its crystallization. This resulted in well-defined, nanostructured assemblies of composite radical crystals (**bTbk**/toluene/C_{60} or C_{70}) or (**bTbk**/toluene/TEMPO) by a very simple dissolution/crystallization process with tunable guest content. Selective C_{60} extraction was also demonstrated directly from fullerene soot.

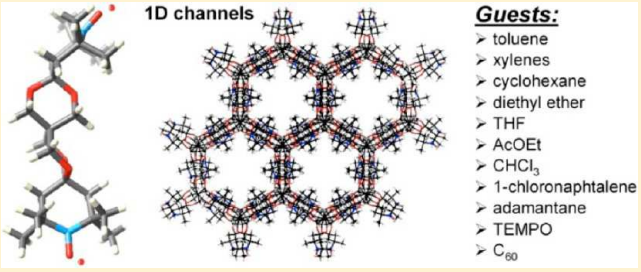

1. INTRODUCTION

The research field of crystalline solids has recently witnessed the emergence of new classes of compounds with the promise of numerous and exciting applications. Although the idea of being able to predict or control the outcome of the arrangement of molecules according to their molecular structure is quite old,[1] this is only recently that some success was reached. In these attempts to control the supramolecular solid architectures, the term "supramolecular synthon" was introduced[2] as some others like "crystal engineering"[3] and "molecular tectonics".[4] Several research groups succeeded in this direction with the construction of organic crystals with predictable arrangements at the nanoscopic level, e.g., crystals with engineered pore sizes,[5] functions introduced at the molecular level,[6] or with the fabrication of hybrid solids as drug carriers.[7] In this vein, a few purely organic compounds based on open shell molecules have been shown to crystallize with open frameworks amenable to guest inclusion.[8,9] However, such clathrate compounds generally possess little void spaces and exhibit reduced robustness upon guest removal.[10] Moreover, as far as we know, the inclusion of functional molecules in large pores has also not been demonstrated for crystals based on organic free radicals.[11] During the past decade, Veciana and co-workers have reported various studies based on chlorotriphenylmethyl radicals as multitopic synthons.[9,11] However, little attention has been devoted to the use of nitroxides for similar assemblies.[12] Nitroxides constitute a well-known family of free radicals characterized by a $\pi_{N-O\bullet}$ three-electron bond including a large number of stable radicals such as 2,2,6,6-tetramethylpiperidinyloxy (TEMPO) (Scheme 1).

Because of their magnetic, chemical, and redox properties, stable nitroxides have received considerable attention[13] and are used in a number of applications, such as in site directed spin labeling (SDSL),[14] molecular magnets,[15] spin probing,[16] spin

Received: July 19, 2013
Revised: December 3, 2013
Published: December 10, 2013

dx.doi.org/10.1021/cg401097e | *Cryst. Growth Des.* 2014, 14, 467−476

Scheme 1. Structures of TEMPO and bTbk

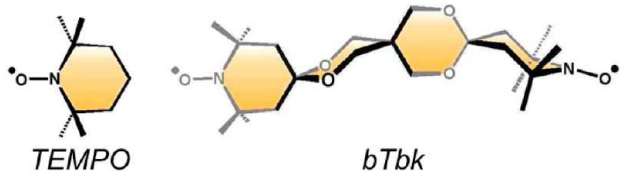

trapping,[17] controlled free radical polymerization,[18] and various imaging techniques.[19] We initially developed the rigid dinitroxide biradical bis(TEMPO) bisketal (**bTbk**) as a polarizing agent for dynamic nuclear polarization (DNP)−solid-state NMR applications.[20] Besides its high performance as a DNP polarizing agent, we recently reported the strong tendency of **bTbk** to gel organic solvents induced by perturbing stimuli,[21] or to afford hybrid crystals with host/guest, isostructural open frameworks.[22] In this paper, we report the structural features of **bTbk** open frameworks with 1D channels formed by the one-dimensional packing of large pockets available for the sequestration of a large variety of molecules in the radical host matrix. This property has been used to easily fill the crystalline pockets with several guests, such as adamantane, C_{60}, C_{70}, and paramagnetic molecules (TEMPO and 2-azaadamantane-*N*-oxyl), and access magnetic organic open frameworks with potentially unique properties endowed by the particular features of the radical walls and of the included guests.

2. EXPERIMENTAL SECTION

2.1. Crystal Growth and Single-Crystal X-ray Diffraction. **bTbk** was prepared according to a previously reported procedure.[20d] The toluene and cyclohexane solvates were obtained from **bTbk** solutions (10 mg) in 10 mL of the relevant solvent. The crystallization can easily be scaled up by 30 times (300 mg/300 mL). The *o*-, *m*-, and *p*-xylene solvates were obtained by slow evaporation of a **bTbk** solution (20 mg) in 10 mL of the corresponding solvent. The ether, hexadecane, and THF solvates were obtained after dissolution of 15 mg of **bTbk** in 10 mL for diethyl ether and hexadecane and 5 mL for THF, which likely contained water, as found by elemental analysis of the **bTbk**/THF solvate. The 1-chloronaphthalene solvate was obtained by slow cooling of a supersaturated **bTbk** solution (510 mg in 12 mL) that was first heated to ∼80 °C. For the adamantane/toluene ternary clathrate, a 3 mL saturated solution of adamantane in toluene was prepared before adding 30 mg of **bTbk**, followed by slow evaporation at room temperature. Crystal growth conditions are given in the text for fullerenes with saturated solutions used for getting crystals with the highest content of fullerenes. The protocol for getting crystals with C_{70} was the same as that used for C_{60}. All crystals were measured on a Bruker-Nonius Kappa CCD diffractometer with the Mo(Kα) radiation. Data reductions were performed with denzo-SMN, and structures were solved by direct methods and refined with SHELXl97. For the open framework crystals, more than 30 attempts were made with different **bTbk**/solvent combinations but we were able to locate the highly disordered guest in the case of toluene only at 100 K. Crystallographic data are summarized in the Supporting Information (Tables S1 and S2).

2.2. Powder X-ray Diffraction. XRD (X-ray diffraction) patterns on powders or crystals were recorded on a Siemens D500R XRD diffractometer using Cu Kα radiation in the 5−40° 2θ range with a 0.04° step associated with a step time of 1 s.

2.3. Thermogravimetric Analysis. Thermogravimetric measurements were performed on a TGA Q500 apparatus (TA Instruments) using air as carrier gas. The samples (∼20−30 mg) were heated up to 500 °C using a simple ramp of 10 °C·min^{-1}.

2.4. Elemental Analysis. The unit cell of the toluene solvate showed the presence of 12 **bTbk** molecules for 4 spherical holes, which makes a **bTbk**/cavity ratio of **3**/1. We then assumed three **bTbk** molecules in the calculations and included increasing amounts of the guests until the fit between the experimental and calculated values of each percentage was satisfactory. The calculated values are given below in parentheses:

bTbk (**1**), C 62.79 (62.70), H 9.37 (9.15), N 6.19 (6.36).
bTbk/*toluene* (**3**/*4.8*), C 69.89 (69.86), H 9.29 (9.05), N 4.73 (4.76).
bTbk/*cyclohexane* (**3**/*4.2*), C 67.39 (67.54), H 10.58 (10.25), N 4.88 (5.02).
bTbk/*1-chloronaphthalene* (**3**/*3.9*), C 66.51 (66.31), H 7.86 (7.59), N 4.20 (4.30).
bTbk/*o-xylene* (**3**/*4.8*), C 70.42 (70.44), H 9.45 (9.25), N 4.47 (4.59).
bTbk/*m-xylene* (**3**/*4.5*), C 70.35 (70.08), H 9.66 (9.24), N 4.82 (4.67).
bTbk/*p-xylene* (**3**/*4.5*), C 70.05 (70.08), H 9.45 (9.24), N 4.61 (4.67).
bTbk/*diethyl ether* (**3**/*3.9*), C 62.77 (63.08), H 10.14 (9.95), N 5.08 (5.22).
bTbk/*THF*/H_2O (**3**/*6*/*1.2*), C 62.85 (62.90), H 9.68 (9.67), N 4.69 (4.73).
bTbk/*adamantane*/*toluene* (**3**/*1*/3), C 69.25 (69.10), H 9.30 (9.28), N 4.85 (4.88).
bTbk/*TEMPO*/*toluene* (**3**/*1*/*4*), C 68.94 (68.95), H 9.35 (9.28), N 5.13 (5.31).
bTbk/*TEMPO*/*1-ClN* (**3**/*2*/*3.4*), C 66.41 (66.44), H 8.37 (8.28), N 5.10 (5.12).
bTbk/*2-azaada.-N-oxyl*/*1-ClN* (**3**/*1*/*4.5*), C 66.93 (66.96), H 7.74 (7.56), N 4.46 (4.44).
bTbk/C_{60}/*toluene* (**3**/*0.05*/*4.8*), C 70.41 (70.46), H 9.07 (8.87), N 4.63 (4.67).
bTbk/C_{60}/*1-ClN* (**3**/*0.18*/*3.1*), C 68.00 (68.04), H 7.40 (7.30), N 4.18 (4.30).
bTbk/C_{70}/*1-ClN* (**3**/*0.05*/*3.7*), C 66.88 (66.90), H 7.75 (7.40), N 4.22 (4.28).

2.5. EPR Spectroscopy. The crystal EPR measurements were performed on a BRUKER EMX spectrometer operating at 9.4 GHz (X-band). The spectrometer was equipped with an Oxford Instruments continuous He-flow cryostat, enabling measurements in the temperature range of 4−300 K. The spectrometer was also equipped with a goniometer, which allowed us to select a precise orientation for the sample. The liquid EPR measurements were performed on a BRUKER Elexsys and EMX spectrometers operating at 9.4 GHz (X-band) in 50 μL capillaries using the following parameters: microwave power, 5 mW, and modulation amplitude, 0.1 G.

3. RESULTS AND DISCUSSION

3.1. bTbk Open Framework: Toluene Clathrate at 213 and 100 K. When hot toluene solutions of **bTbk** were cooled to room temperature, large orange crystals formed belonging to the $R\bar{3}$ trigonal space group. At 213 K, there are two molecules in the asymmetric unit, one of **bTbk** and one of toluene. Expansion to the unit cell showed that the dinitroxide self-assembles into a honeycomb hexagonal structure with one-dimensional channels including several toluene molecules (Figure 1a).[21,22] The solvent is clustered in pockets of approximate dimensions of ∼11.4 × 11.4 × 12.2 Å (see Figures 1 and 6) and disordered over several sites. A molecule of toluene was fixed in the asymmetric unit during the refinement cycles before converging to a partial occupancy of 0.33 for 0.5 molecule of **bTbk** with unit cell parameters $a = b =$ 25.104 Å and c = 30.000 Å. This procedure afforded the following composition of 3 **bTbk** for 2.1 toluene molecules with a reasonably good agreement factor of 0.0810. However, because of the guest disordering, the crystal composition may not be entirely accurate, and thus, we recorded single-crystal X-

dx.doi.org/10.1021/cg401097e | Cryst. Growth Des. 2014, 14, 467−476

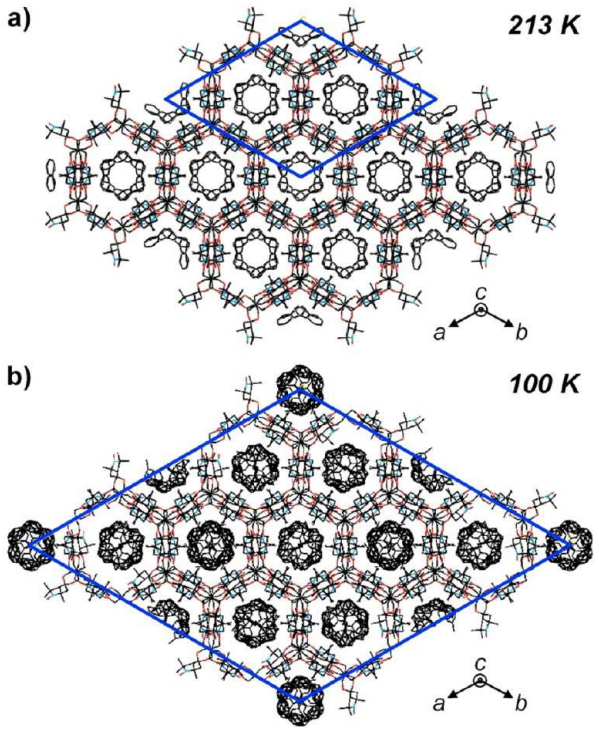

Figure 1. Single-crystal X-ray structures obtained (a) at 213 K and (b) at 100 K. Note the guest ordering phenomenon observed at 100 K that causes the unit cell parameters to be twice as those of the structure with disordered toluene in the channels (213 K). Hydrogen atoms are omitted for clarity.

ray data at 100 K. In this case, a phenomenon of guest ordering[23] was observed with some positions of the toluene molecules now identifiable (Figure 1b). Then, even though, at 100 K, the **bTbk** framework is virtually identical, decreasing the temperature resulted in symmetry lowering regarding guests arrangement and caused the doubling of unit cell parameters *a* and *b*. The agreement factor is slightly higher (0.0937), but the composition, 3 **bTbk** for 4.5 toluene molecules, is now in very good agreement with the ones determined by elemental analysis (3 **bTbk** for 4.8 toluene molecules) and by TGA (3 **bTbk** for 5.0 toluene molecules; see below). From these data, the **bTbK** open framework can accommodate approximately 30 wt % of toluene.

3.2. bTbk Open Framework: Relevance of CH···•ON Interactions. The **bTbk** open framework is maintained by multiple CH···•ON interactions.[24] Indeed, a close look at the structure shows a number of 12 H-bond interactions per **bTbk** molecule (Figure 2a), four of which are rather strong (C−H···O: 2.43 Å, 172°) and eight somewhat weaker (C−H···O: ∼2.62 Å, 152°).[25]

To get a global view of the intermolecular interactions in the crystal, we decided to plot the Hirshfeld surfaces[26] and map the d_{norm} parameter using the software CrystalExplorer (Figure 2b).[27] The d_{norm} parameter represents a contact distance of atoms of the considered molecule (inner to the Hirshfeld surface) with respect to the ones of neighboring molecules in the crystal (outer to the Hirshfeld surface). This program enables an easy visualization of intermolecular close contacts in crystals. Red areas (contacts) are easily identified on the nitroxyl oxygen atoms at the periphery of the **bTbk** skeleton (H bond acceptors) and for hydrogen atoms of the dioxane methylene groups (H bond donors, Figure 2b), thus confirming the above-mentioned observation (Figure 2a). From this mapping, all close contacts have been quantified and, apart from an important contribution of H−H contacts likely due to the packing, the CH···•ON interactions are the only others in the crystals. CH···•ON interactions are thus ubiquitous in this structure and are responsible for the network assembly and, to some degree, to the partial stability of the architecture. It is very likely that these structurally determining H bonds are strong due to the high dipolar moment of the nitroxide group (3.14 D; see Scheme 2)[28] and the pseudoacidic character of the methylene hydrogen atoms adjacent to the dioxane ketal oxygen atoms.

Noteworthily, no single crystals have been obtained with the diamine precursor of **bTbk**, highlighting the role of the nitroxide moieties in the crystal assembly.

Therefore, it appears that the orthogonal and rigid structure of **bTbk** induces a strong directional positioning of the

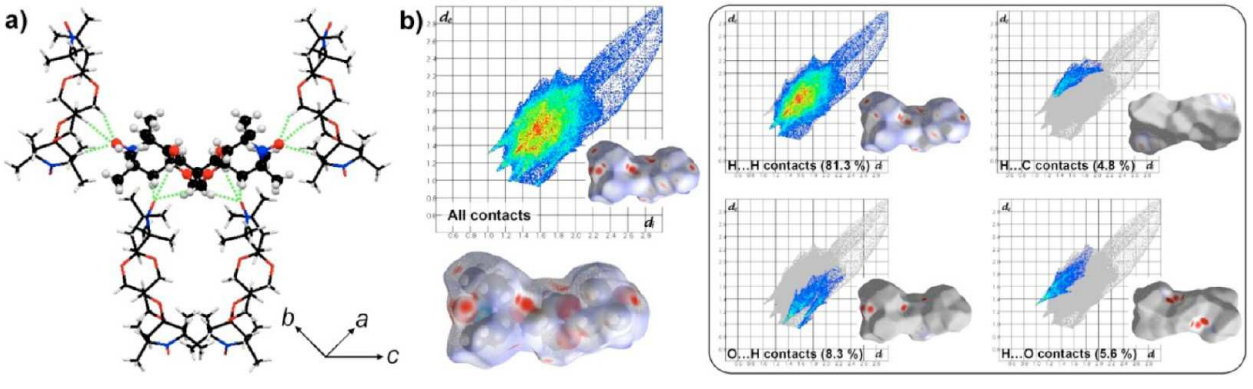

Figure 2. (a) Multiple CH···•ON interactions surrounding one **bTbk** molecule. (b) Hirshfeld surface analysis of **bTbk** in the crystal structure of the toluene solvate (the guests were removed to account for the interactions within the open framework). A large part of the **bTbk** surface is engaged in H···H contacts while the two extremities (N−O• bonds) and the concave surfaces (C−H bonds) are engaged in strong CH···•ON interactions. The d_e versus d_i diagram illustrates the close contacts between the considered molecule (**bTbk**) and surrounding molecules in the crystal (other **bTbk** molecules of the framework). For each case where two atoms are sufficiently close, d_e represents the distance between the Hirshfeld surface (positioned in between the two atoms) and the external atom and d_i stands for the distance between the Hirshfeld surface and the internal atom. (Part a: Reproduced by permission of The Royal Society of Chemistry: http://pubs.rsc.org/en/content/articlelanding/ra/2012/c2ra20208e#!divAbstract).

dx.doi.org/10.1021/cg401097e | *Cryst. Growth Des.* 2014, 14, 467−476

Scheme 2. Main Resonant Structures of the Aminoxyl Function

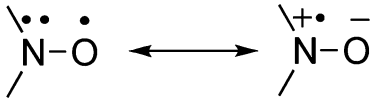

interacting groups (NO• and slightly acidic hydrogen atoms). As a means to establish the strength of these nonclassical H bonds, we studied the crystal structures of a series of dinitroxides (Figure 3).

It appeared that the total number of nonclassical H bonds in which **bTbk** is engaged is the highest in the series, as well as the number of strong H bonds.[25] With a quasi-equal number of interactions of the CH···•ON type (2 strong and 8 weak), dinitroxide **dCdO**[29] crystallizes also with one-dimensional channels. The structure of dinitroxide **Isoindoxazo**[30] has water and a bromide counterion in which there are six CH···Br interactions, thus precluding the formation of a high number of CH···•ON interactions. The situation is similar for **Tycio**[30] in which there are competitive H bonds involving the amide groups, thus decreasing the contribution of CH···•ON interactions. In the sulfur analogue **bTbkS4**,[31] the interactions are weaker due to the replacement of O atoms by S atoms. **bTbkS4** crystallizes with molecules arranged pairwise and further stack in two-dimensional sheets that pack on one another. In the case of **bCdO**[30] and **bTurea**,[29] CH···•ON interactions are still present, but to a lower extent. Such interactions in **ADTP**[32] and **Tempoxazo**[30] are, respectively, classified as modest and strong, but again, their number is not sufficient to compare favorably with those of **bTbk**.

3.3. bTbk Open Frameworks: Organic Solvent Clathrates. The crystals of 16 solvates were studied by single-crystal X-ray diffraction, and all exhibited the open framework structure (Table 1). The channel structure is always obtained ($R\bar{3}$ space group) except in ethanol, water, and hexadecane.[33] Thus, it seems that the rigid scaffold of **bTbk** with suitable functions endowed within the structure encodes for several levels of information (chemical nature of the functional groups and very strict spatial positioning),[34] leading to an open framework containing large pockets that stack in one dimension. As already reported, the multiplication of weak intermolecular interactions (in the absence of competing ones) can be a strong advantage in favoring some molecules to self-assemble in predetermined fashions.[35]

The high number of CH···•ON interactions per **bTbk** units is very likely to be at the origin of the observed open framework, but the structure stability is also dependent on the included guest (with a time scale from minutes to several months). For instance, over a few hours, the bright orange toluene solvate crystals turned opaque when taken out of the toluene solutions (see Figure 4). Elemental analysis no longer showed toluene molecules in the material (**bTbk** alone), which structurally changed to a new phase (see PXRD, Figure 4, and scanning electron microscopy, Figure S1, Supporting Information).

Powder X-ray diffraction (PXRD) showed that the structure collapses upon solvent (guest) evaporation with various kinetics depending on the included guest molecules but also that it can be strengthened by inclusion of appropriate guests (Table 1). The PXRD pattern of this opaque material is in good agreement with the calculated pattern of a **bTbk** single crystal grown in water in which no channels are observed (dense phase; see Table 1, Figure 4, and the Supporting Information). These results show that the escape of toluene molecules from the channels causes the structure to collapse to a polycrystalline powder structurally ordered as in the dense phase (see the Supporting Information for the single-crystal X-ray diffraction data of the dense phase). As shown in Table 1, the same behavior is observed with other solvents, but with a guest-dependent stability not correlated to the boiling point or vapor pressure of the solvent. For instance, the cyclohexane and 1-chloronaphthalene solvates exhibit an increased stability from hours to weeks and months, respectively. Interestingly, the same open framework formed in a variety of organic solvents, including hydrogen bond donors and acceptors. The presence of water in THF did not hamper the formation of the channel structure. TGA results are in good agreement with the composition given by elemental analysis for the toluene and cyclohexane solvates and for the material obtained after collapse of the network (see Figure 5). Two types of behaviors are evidenced among all the samples. For solvate phases obtained with toluene or cyclohexane, the weight is constant up to ~40 °C, and then it decreases strongly up to 70 °C (~20–30%). In this region, the toluene and cyclohexane are removed from the channel structure. From 70 °C to ~200–220 °C, there is a further plateau before the weight of the samples

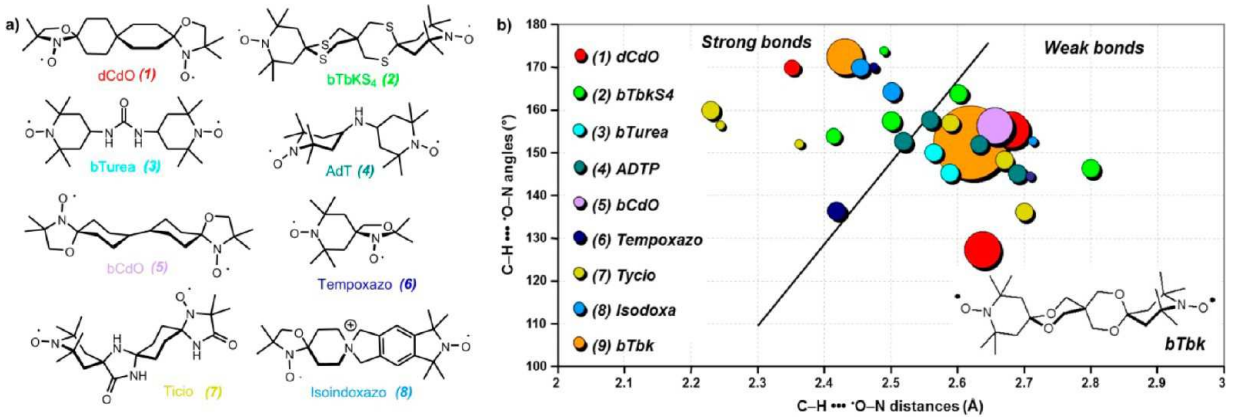

Figure 3. Dinitroxides displaying CH···•ON interactions in the solid state (a), the number and strength of which are shown on the graph (b), per molecule in each crystal structure (the size of the dots directly reflects the number of interactions per dinitroxide).

dx.doi.org/10.1021/cg401097e | Cryst. Growth Des. 2014, 14, 467–476

Table 1. X-ray Structural Features, Stability, Guest Positioning, and Occupancy of bTbk Single Crystals and Cocrystals Obtained with Solvents of Various Polarity and Various Guests

solvent	framework[a]	guest	stability	N_{guest}[b]
1-Cl-naphthalene	channels	unresolved	months	3.9
cyclohexane	channels	unresolved	weeks	4.2
toluene	channels	located	hours	4.8
o-xylene	channels	unresolved	hours	4.8
m-xylene	channels	unresolved	days	4.5
p-xylene	channels	unresolved	hours	4.5
Et_2O	channels	unresolved	hours	3.9
THF/H_2O	channels	unresolved	days	6/1.2
AcOEt	channels	[c]	minutes	5.3[d]
$CHCl_3$	channels	[c]	hours	5.0[d]
toluene/adamantane	channels	unresolved	hours	3/1
toluene/TEMPO	channels	unresolved	hours	4/1
1-Cl-naphthalene/TEMPO	channels	unresolved	months	3.4/2
1-Cl-naphthalene/2-azaNO	channels	unresolved	months	4.5/1
toluene/C_{60}	channels	unresolved	days	4.8/0.05
1-Cl-naphthalene/C_{60}	channels	unresolved	months	3.1/0.18
EtOH	dense	no	months	
water	dense	no	months	
hexadecane	dense	no	months	

[a]Crystallographically determined using single crystals (T = 213 or 293 K). [b]Number of included guest molecules per cavity as estimated by elemental analysis. [c]Not determined. [d]Determined by TGA.

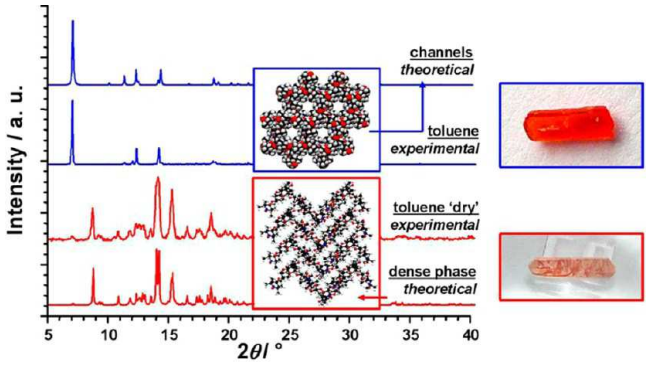

Figure 4. X-ray diffraction (XRD) patterns of gently ground freshly prepared **bTbk** crystals (toluene experimental) and the same crystals of the toluene solvate after drying (toluene "dry" experimental). The top and the bottom patterns are theoretical traces derived from the single-crystal X-ray diffraction data of the channel structure and that of the dense phase, respectively.

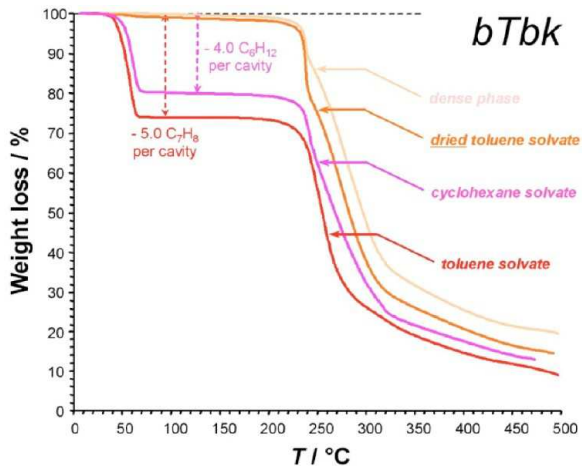

Figure 5. TGA traces of the dense phase and the toluene and cyclohexane solvates.

decreases again up to the almost total decomposition of the organic network. For the dense phase (obtained after SiO_2 chromatography column or after drying of the toluene solvate), there is only one weight loss phenomenon that is evidenced: it starts around 210 °C and ends at 500 °C corresponding to the almost total decomposition of the organic network. Note that the TGA trace of the dried toluene solvate is in good agreement with that of the dense phase.

The amount of solvent estimated from TGA and elemental analysis (EA) is very close for cyclohexane (4.0 C_6H_{12} per cavity instead of 4.2 by EA) and for toluene (5.0 C_7H_8 per cavity instead of 4.8 by EA). The high quantity of toluene (around 5 molecules per 3 **bTbk**) in the crystals could be a reason for their metastability. We used a rationale of 3 **bTbk** per cavity when indicating the number of included guests (N_{guest}, Table 1) since there are 4 pockets per unit cell, which also contains 12 **bTbk** molecules.

3.4. bTbk Open Frameworks: Inclusion of Functional Guests. A careful examination of the pocket architecture of the channels revealed a lipophilic environment (bowl shape with hydrogen atoms of C−H bonds pointing inward) suitable for the inclusion of hydrophobic guests (Figure 6, top). To evaluate the possible preparation of functional crystals, we reasoned that a size complementary guest like adamantane (~7.2 Å diameter) could be included in the host framework (approximate size of the pockets ~11.4 × 11.4 × 12.2 Å). Ternary orange crystals of **bTbk**/adamantane/toluene were obtained after slow cooling of an adamantane saturated solution of **bTbk** in toluene. Single-crystal X-ray diffraction showed the dinitroxide open framework, but the position of the guests could not be resolved. Elemental analyses indicated the presence of toluene and adamantane in a 3/1 ratio (Table 1). However, incorporation of adamantane as a stopper is not sufficient to prevent the collapse of the framework due to the toluene escape. This observation highlights a peculiar flexibility

dx.doi.org/10.1021/cg401097e | Cryst. Growth Des. 2014, 14, 467−476

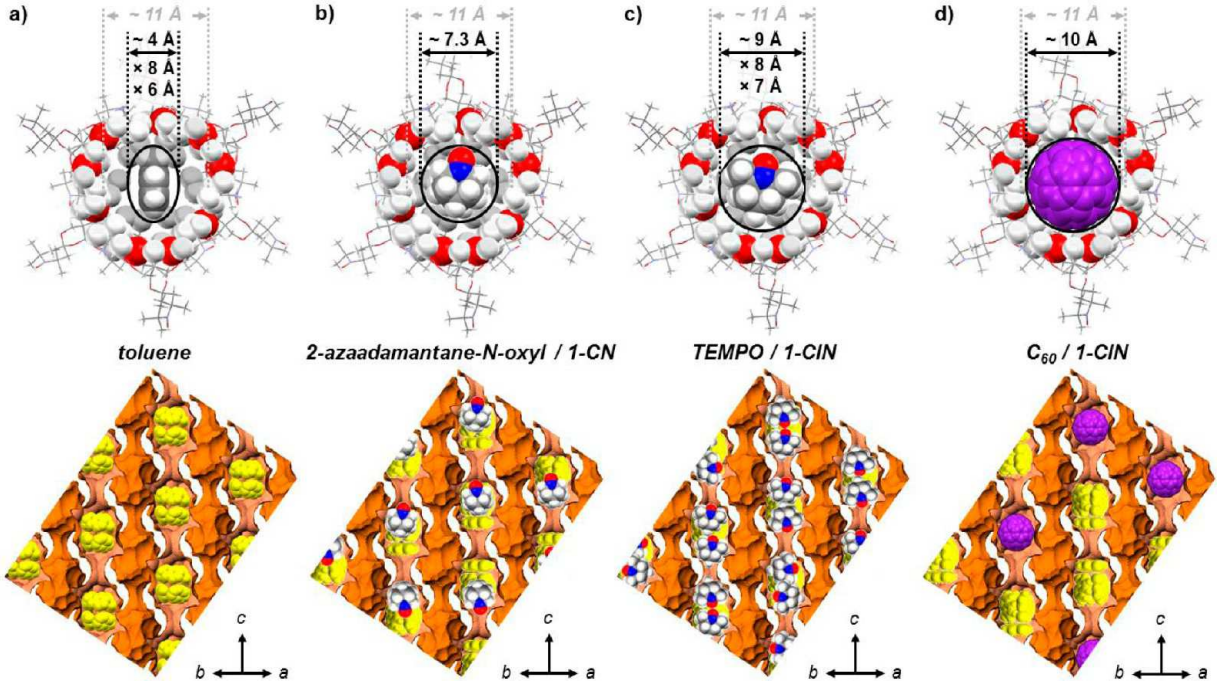

Figure 6. Top line: view of the hydrophobic environment of one-half-pocket belonging to the 1D channels of the **bTbk** open framework crystals, as depicted by space-filling mode of the atoms positioned along the **bTbk** skeleton that form a bowl space for guest accommodation. The approximate sizes of toluene (a) and solid guests such as 2-azaadamantane-*N*-oxyl (b), TEMPO (c), and C_{60} (d) are given with respect to the dimensions of the pockets (~11.4 × 11.4 × 12.2 Å) inside the channels of the **bTbk** open framework.[21] The bottom line displays X-ray derived pictures of the channels' shape (dark orange, cross section in salmon-pink) and of the included guests (highly disordered), in agreement with elemental analysis and TGA (see text and Table 1 for further information; the positions of included free radicals and of C_{60}, respectively, in (b)−(d) are only one particular example for a situation in which guests are randomly positioned in the pockets of the channels). (Parts a and d, bottom: Reproduced by permission of The Royal Society of Chemistry: http://pubs.rsc.org/en/content/articlelanding/2013/cc/c3cc00170a#!divAbstract).

of the **bTbk** framework to evolve to the thermodynamically stable dense phase.[36] Indeed, the smallest cross section of the channels at the bottleneck is around 4.4 Å. Toluene molecules (7.7 × 6.4 Å) can still escape through these constricted channels. This observation shows that the X-ray derived structure of these single crystals should not be regarded as a fixed picture but with a dynamic component, which is still difficult to visualize and to quantify.

To determine whether the inclusion of more appealing *functional* guests could be realized, the inclusion of the stable radical TEMPO was studied. At first sight, the formation of the **bTbk** framework in the presence of large quantities of TEMPO would have seemed unlikely due to the similarities between the host and the guest structures. Indeed, one would expect TEMPO to compete for the self-assembly during crystal growth. However, bright orange crystals of **bTbk** (50 mg) formed in toluene (300 μL) in the presence of TEMPO (100 mg) after dissolution and crystallization ($R\bar{3}$ space group). Elemental analysis is in line with the following composition: **bTbk**/toluene/TEMPO (3/4/1), which makes 4 toluenes and 1 TEMPO per cavity. HPLC analysis of dissolved crystals clearly showed a mixture of TEMPO and **bTbk** (Figure S4, Supporting Information). To obtain more stable crystals, 1-chloronaphthalene was used as solvent (450 mg of TEMPO for 150 mg of **bTbk**). New orange crystals formed enriched in TEMPO since they now count 2 TEMPO and 3.4 1-chloronaphthalene molecules per cavity, as determined by elemental analysis (Figure 6c). We believe that the forces responsible for the **bTbk** solid-state self-assembly (12 H bonds per molecule) are stronger than the potential interactions of **bTbk** with TEMPO. The robustness of crystal growth affording always the same open framework despite a number of variations in the experimental conditions is remarkable. We used this property to also include a larger free radical: 2-azaadamantane-*N*-oxyl in 1-ClN (Figure 6b). Remarkably, single crystals of the open framework were again obtained with one radical per pocket (elemental analysis derived composition: **bTbk**/1-ClN/2-azaadamantane-*N*-oxyl: 3/4.5/1). In the two cases, the nitroxide position could not be resolved by single-crystal XRD. We then wondered what could be the maximum size of a guest to be included inside this matrix. Because of the spherical shape of the pockets, fullerenes C_{60} and C_{70} appeared to be interesting candidates[37] due to their photophysical properties. C_{60} and C_{70} can be included successfully in the **bTbk** paramagnetic matrix and homogeneously stained isostructural purple, and brown crystals, were obtained respectively. For adamantane, TEMPO, or 2-azaadamantane-*N*-oxyl, all the pockets of the channels are occupied with one or two of these guest molecules. However, for fullerenes, the best inclusion percentage that could be obtained (20%), was for C_{60} in 1-ClN. Purple crystals formed overnight after slow cooling of a hot concentrated solution (3.2 mL) of **bTbk** (120 mg) and C_{60} (160 mg). This result may be due to the limited C_{60} solubility or to some steric constrains during crystal growth since the size of this fullerene (~10.3 Å diameter) almost reaches the limit value of what can be included in the pockets. Actually, the maximum size for a sphere fitting the pockets is for a diameter of ~9 Å, as estimated by ATOMS. This would mean that there can be some reasonable degrees of freedom to accommodate large guests, but the cage is quite rigid and the

dx.doi.org/10.1021/cg401097e | *Cryst. Growth Des.* 2014, 14, 467−476

inclusion of even larger guests would presumably not be possible because of the energy cost of perturbing the proper self-assembly of the stabilizing network of CH···O interactions.

Elemental analysis allowed determining that 1 site over 5 is occupied by a C_{60} molecule (~20% of the pockets do contain C_{60} while the remaining space is filled with 1-chloronaphthalene). We note that, when using 1-chloronaphthalene instead of toluene, the C_{60} percentage of inclusion per cavity reaches 20 instead of ~5 (Figure 6d). We previously showed that the very strong fidelity of **bTbk** to crystallize according to the channel structure was used to prepare the first organic multishell isostructural host/guest crystals (with a free radical and C_{60}).[22] In the case of C_{70}, this percentage is maintained around 5 whatever the solvent, which means that we probably reached the limit in terms of the size. These results suggest possible size selectivity in fullerene inclusion inside **bTbk** open framework single crystals (see the following section).

3.5. bTbk Open Frameworks: Selective Extraction of Fullerene C_{60}. Because of the preference for the open framework to include C_{60} versus C_{70} and because **bTbk** crystallizes even in complex media, we tried to crystallize the biradical directly from the commercially available fullerene soot (7 wt % C_{60}/C_{70} fullerenes). Our aim was to check if (i) **bTbk** still crystallized according to the channel motif, (ii) fullerenes could still be entrapped in these conditions and, if so, (iii) to which extent. Fullerene soot (1.5 g) was added to a solution of **bTbk** (780 mg) in 1-ClN (20 mL). After heating at 80 °C for 15 min, the suspension was allowed to cool to room temperature and 280 mg of dark crystals were collected after 1 week (Figure 7, inset). Each crystal was carefully cleaned with a few drops of 1-ClN to clean the crystals' faces (channel structure).

For determining what the framework contained, the following procedure was used: 200 mg of dark crystals were introduced in a 1.5 mL vial before addition of methanol (1 mL) and exposure to ultrasound for 2 min. The resulting dark suspension was then centrifuged for 5 min and allowed to collect a dark precipitate while the methanolic supernatant containing **bTbk** and 1-ClN was separated. The dark precipitate was then washed this way three more times before elimination of the remaining methanol at 60 °C under reduced pressure.

The ^{13}C NMR spectrum in d_4-orthodichlorobenzene (ODCB) showed one major resonance peak at 142.84 ppm (C_{60}, Figure 7a). No additional signals attributable to C_{70} and possible aromatic low-molecular-weight species (fullerene soot) were observed. MALDI-TOF MS spectra showed only one peak at m/z = 720.0 amu (Figure 7b). It is noteworthy that the same MS analysis of a commercial C_{60}/C_{70} mixture (75/25) exhibited a 1 to 1 peak ratio (Figure 7, inset, and for fullerene soot extracts, Figures S2 and S3, Supporting Information) for C_{60} and C_{70}. These experiments indicate a selective inclusion of C_{60} vs C_{70}. Single crystals have unit cell parameters identical to those of the open framework, and elemental analyses of the dark crystals are in agreement with a percentage of C_{60} inclusion between 9 and 12, which is comparable to what was obtained with **bTbk** crystallized from pure C_{60}. The present selective extraction method afforded 10 mg of pure C_{60}, which gives a yield of ≈25% of C_{60} recovery directly from the soot. Despite a limited capacity of C_{60} inclusion in the open framework, the recovery of C_{60} from fullerene soot is easy and selective and highlights the robustness and high fidelity of crystallization according to the open framework of **bTbk**.

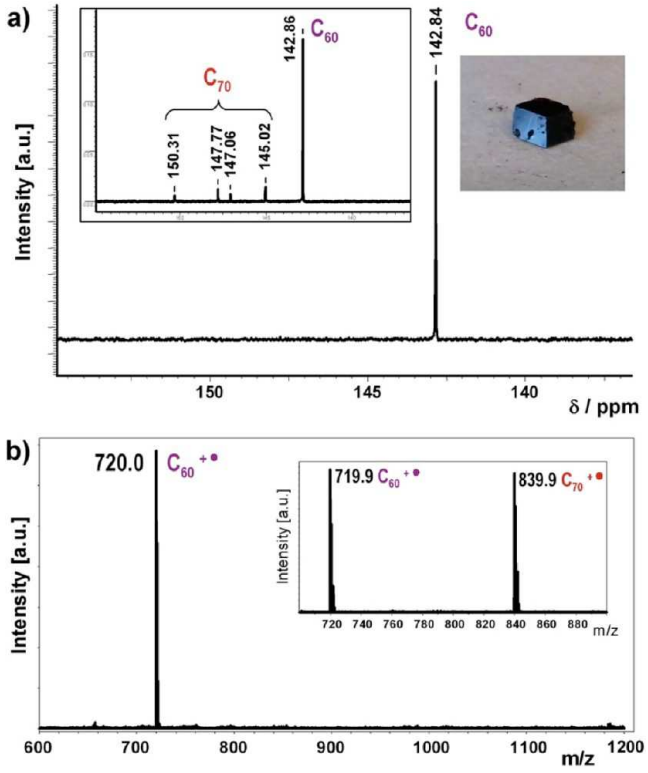

Figure 7. (a) ^{13}C NMR spectrum of the content of the **bTbk** dark crystals after **bTbk** extraction (inset: representative example of a dark crystal and ^{13}C NMR of a commercial C_{60}/C_{70} mixture, 75/25). (b) MALDI-TOF MS spectrum of the same dark product obtained after **bTbk** extraction (inset shows the data obtained from the commercial C_{60}/C_{70} mixture).

3.6. EPR Study of a Toluene Clathrate Single Crystal of bTbk. Owing to the paramagnetic nature of **bTbk**, we used EPR spectroscopy to further characterize the crystals. The X-band EPR spectrum of **bTbk** in toluene (0.5×10^{-3} M) at room temperature is close to that of TEMPO and exhibits three lines with an hyperfine coupling constant of a_N = 15.08 G (g_{iso} = 2.0064(3)).[38] In a previous study,[38] it has been determined that the spin exchange coupling is negligible compared to the hyperfine coupling (a_N). A variable-temperature EPR study of a toluene solvate of a **bTbk** crystal was performed to evaluate the magnetic properties of the **bTbk** open framework. The magnetic susceptibility (χ) was measured between 4 and 200 K with an X-band EPR spectrometer. The acquired EPR spectra, which were recorded in the form of the derivative of absorption with respect to the magnetic field H, can be well-fitted by the Lorentzian function with a typical line width of a few Gauss (Figure 8).

The behavior of the temperature dependence of the static susceptibility of **bTbk** (crystal of the toluene solvate), as determined from a double integration of the EPR signal, is well reproduced by a Curie law expressed by $\chi = C/T$, as shown in Figure 8. These results showed that **bTbk** in the solid-state phase at temperatures above 4 K can be described as an ensemble of almost isolated paramagnetic centers with a negligibly small exchange interaction.

4. CONCLUSION

In summary, we have discovered the clear tendency of a rigid spiro dinitroxide biradical (**bTbk**) to crystallize in a variety of

dx.doi.org/10.1021/cg401097e | Cryst. Growth Des. 2014, 14, 467−476

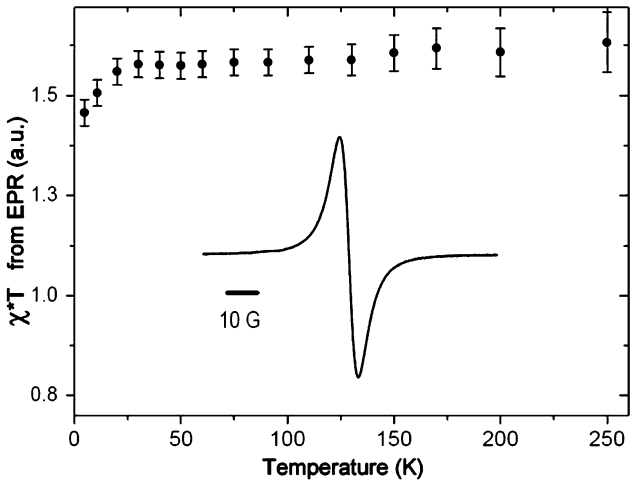

Figure 8. Variable-temperature study of the magnetic susceptibility of a toluene solvate of the open framework crystal of **bTbk** (inset shows the EPR spectrum at room temperature).

experimental conditions forming an open framework with versatile corrugated 1D channels, which can be described as a 1D stacking of nanoreservoirs. It is remarkable that this dinitroxide biradical exhibits such a strong tendency to form a unique open framework whose structure is maintained by multiple weak CH···•ON interactions, highlighting the role of the nitroxide function as a potential useful building block for supramolecular assemblies.[39] This behavior can be paralleled with a series of pentaerythritol bisketal compounds that also crystallized with a variety of channel shapes.[40] The absence of such structural properties in the corresponding diamine of **bTbk** strongly suggests that the nitroxide moieties are pivotal for such an assembly and could be an interesting component for crystal engineering. The fact that the open framework was obtained in a large variety of solvents and of experimental conditions was used to include several functional guests, such as TEMPO and fullerenes C_{60} and C_{70}. Well-defined, nanostructured assemblies of composite radical crystals made up of a **bTbk** paramagnetic framework with included TEMPO or fullerenes can be accessed very easily by a simple dissolution/crystallization process with tunable guest content. The properties of the C_{60}@**bTbk** crystal will be investigated under laser irradiation in order to evaluate the magnetic interactions between the triplet excited state of fullerene C_{60} and **bTbk**. The structural features that both include strong directional positioning and multiple CH···•ON interactions bode well for further discoveries and applications of nitroxides in multifunctional crystals. For instance, the demonstration of the sequestration of TEMPO or 2-azaadamantane-*N*-oxyl radical in ordered well-defined **bTbk** cavities resulted in nanostructured assemblies of a radical in an organic paramagnetic crystal (**bTbk** biradical). The inclusion of paramagnetic guests in diamagnetic matrixes seems to be the subject of recent intense investigations.[41] We are now investigating the magnetic properties and the possibility to include other guests to explore the use of **bTbk** open frameworks as crystalline molecular flasks.[42]

■ ASSOCIATED CONTENT

Ⓢ Supporting Information

HPLC, SEM, additional MALDI spectra, and crystal structure data are supplied in the Supporting Information. CCDC numbers, dense phase: 794600, toluene solvate 100 K, 923774. This material is available free of charge via the Internet at http://pubs.acs.org.

■ AUTHOR INFORMATION

Corresponding Author

*E-mail: david.bardelang@univ-amu.fr. Fax: (+33) 491 288 758.

Present Address

▽Dr. Md. B. Zaman, AB-Biotech Inc., National Research Council of Canada, 100 Sussex Drive, Ottawa, Ontario K1A 0R6, Canada.

Notes

The authors declare no competing financial interest.

■ ACKNOWLEDGMENTS

CNRS, Aix-Marseille Université, and the National Research Council of Canada are acknowledged for financial support. Dr. Md. B. Zaman acknowledges the visiting professor program, King Saud University, Riyadh 11421, Saudi Arabia, for financial support. We also acknowledge Alain Garnier and Emily Bloch for measurements on the open framework, Gregory Excoffier for elemental analyses, and Hakim Karoui for solid-state EPR measurements.

■ REFERENCES

(1) Maddox, J. *Nature* **1988**, *335*, 201.
(2) (a) Desiraju, G. R. *Angew. Chem., Int. Ed.* **2007**, *46*, 8342−8356. (b) Desiraju, G. R. *Angew. Chem., Int. Ed. Engl.* **1995**, *34*, 2311−2327.
(3) (a) Wuest, J. D. *Chem. Commun.* **2005**, 5830−5837. (b) Hosseini, M. W. *Chem. Commun.* **2005**, 5825−5829. (c) Ward, M. D. *Chem. Commun.* **2005**, 5838−5842. (d) Moulton, B.; Zaworotko, M. J. *Chem. Rev.* **2001**, *101*, 1629−1658.
(4) (a) Dechambenoit, P.; Ferlay, S.; Kyritsakas, N.; Hosseini, M. W. *J. Am. Chem. Soc.* **2008**, *130*, 17106−17113. (b) Malek, N.; Maris, T.; Perron, M.-E.; Wuest, J. D. *Angew. Chem., Int. Ed.* **2005**, *44*, 4021−4025. (c) Hosseini, M. W. *Acc. Chem. Res.* **2005**, *38*, 313−323. (d) Laliberté, D.; Maris, T.; Sirois, A.; Wuest, J. D. *Org. Lett.* **2003**, *5*, 4787−4790. (e) Wang, X.; Simard, M.; Wuest, J. D. *J. Am. Chem. Soc.* **1994**, *116*, 12119−12120.
(5) Eddaoudi, M.; Kim, J.; Rosi, N.; Vodak, D.; Wachter, J.; O'Keeffe, M.; Yaghi, O. M. *Science* **2002**, *295*, 469−472.
(6) (a) Yanai, N.; Uemura, T.; Inoue, M.; Matsuda, R.; Fukushima, T.; Tsujimoto, M.; Isoda, S.; Kitagawa, S. *J. Am. Chem. Soc.* **2012**, *134*, 4501−4504. (b) Takashima, Y.; Martinez, V. M.; Furukawa, S.; Kondo, M.; Shimomura, S.; Uehara, H.; Nakahama, M.; Sugimoto, K.; Kitagawa, S. *Nat. Commun.* **2011**, *2*, 168. (c) Kondo, M.; Furukawa, S.; Hirai, K.; Kitagawa, S. *Angew. Chem., Int. Ed.* **2010**, *49*, 5327−5330.
(7) Horcajada, P.; Serre, C.; Maurin, G.; Ramsahye, N. A.; Balas, F.; Vallet-Regi, M.; Sebban, M.; Taulelle, F.; Férey, G. *J. Am. Chem. Soc.* **2008**, *130*, 6774−6780.
(8) Pandian, R. P.; Kim, Y.-I.; Woodward, P. M.; Zweier, J. L.; Manoharan, P. T.; Kuppusamy, P. *J. Mater. Chem.* **2006**, *16*, 3609−3618.
(9) (a) Roques, D. N.; Wurst, K.; Tejada, J.; Rovira, C.; Ruiz-Molina, D.; Veciana, J. *Chem.—Eur. J.* **2007**, *13*, 8153−8163. (b) Roques, N.; Maspoch, D.; Wurst, K.; Ruiz-Molina, D.; Rovira, C.; Veciana, J. *Chem.—Eur. J.* **2006**, *12*, 9238−9253. (c) Maspoch, D.; Domingo, N.; Ruiz-Molina, D.; Wurst, K.; Vaughan, G.; Tejada, J.; Rovira, C.; Veciana, J. *Angew. Chem., Int. Ed.* **2004**, *43*, 1828−1832.
(10) (a) Alavi, S.; Udachin, K.; Ripmeester, J. A. *Chem.—Eur. J.* **2010**, *16*, 1017−1025. (b) Jacobs, T.; Lloyd, G. O.; Bredenkamp, M. W.; Barbour, L. J. *CrystEngComm* **2009**, *11*, 1545−1548. (c) Lu, H.; Seo, Y.-T.; Lee, J.-W.; Moudrakovski, I.; Ripmeester, J. A.; Chapman, N. R.; Coffin, R. B.; Gardner, G.; Pohlman, J. *Nature* **2007**, *445*, 303−306. (d) Swift, J. A.; Pivovar, A. M.; Reynolds, A. M.; Ward, M. D. *J. Am. Chem. Soc.* **1998**, *120*, 5887−5894. (e) Ripmeester, J. A.; Tse, J. S.;

Ratcliffe, C. I.; Powell, B. M. *Nature* **1987**, *325*, 135−136. (f) Hagan, M. M. *J. Chem. Educ.* **1963**, *40*, 643. (g) Mandelcorn, L. *Chem. Rev.* **1959**, *59*, 827−839.

(11) In the following articles, Veciana and co-workers showed that some trityl radicals can be crystallized with significant void spaces arranged in columns defining channels. However, the scope of potential guests inclusion was not studied to the best of our knowledge; see (a) Maspoch, D.; Domingo, N.; Ruiz-Molina, D.; Wurst, K.; Tejada, J.; Rovira, C.; Veciana, J. *J. Am. Chem. Soc.* **2004**, *126*, 730−731. (b) Veciana, J.; Carilla, J.; Miravitlles, C.; Molins, E. *J. Chem. Soc., Chem. Commun.* **1987**, *11*, 812−814.

(12) To the best of our knowledge, a few examples of nitroxide radical crystal structures were reported with included solvent; see: (a) Sawai, T.; Sato, K.; Ise, T.; Shiomi, D.; Toyota, K.; Morita, Y.; Takui, T. *Angew. Chem., Int. Ed.* **2008**, *47*, 3988−3990. (b) Ishida, T.; Ooishi, M.; Ishii, N.; Mori, H.; Nogami, T. *Polyhedron* **2007**, *26*, 1793−1799. (c) Rajca, A.; Pink, M.; Mukherjee, S.; Rajca, S.; Das, K. *Tetrahedron* **2007**, *63*, 10731−10742. (d) Awaga, K.; Wada, N.; Watanabe, I.; Inabe, T. *Philos. Trans. R. Soc. London, Ser. A* **1999**, *357*, 2893−2922. (e) Combet, J.; Morelon, N. D.; Ferrand, M.; Bée, M.; Djurado, D.; Commandeur, G.; Castejon, J. M. *J. Phys.: Condens. Matter* **1997**, *9*, L403−L409 and references therein for the inclusion crystals of TEMPONE.

(13) Bardelang, D.; Hardy, M.; Ouari, O.; Tordo, P. In *Encyclopedia of Radicals in Chemistry, Biology and Materials*; Chatgilialoglu, C., Studer, A., Eds.; Wiley: Chichester, U.K., 2012; Vol. 4, pp 1965−2015.

(14) (a) McCoy, J.; Hubbell, W. L. *Proc. Natl. Acad. Sci. U.S.A.* **2011**, *108*, 1331−1336. (b) Krstic, I.; Hänsel, R.; Romainczyk, O.; Engels, J. W.; Dötsch, V.; Prisner, T. F. *Angew. Chem., Int. Ed.* **2011**, *50*, 5070−5074.

(15) (a) Suzuki, S.; Furui, T.; Kuratsu, M.; Kozaki, M.; Shiomi, D.; Sato, K.; Takui, T.; Okada, K. *J. Am. Chem. Soc.* **2010**, *132*, 15908−15910. (b) Rajca, A.; Takahashi, M.; Pink, M.; Spagnol, G.; Rajca, S. *J. Am. Chem. Soc.* **2007**, *129*, 10159−10170. (c) Rajca, A.; Mukherjee, S.; Pink, M.; Rajca, S. *J. Am. Chem. Soc.* **2006**, *128*, 13497−13507. (d) Dvolaitzky, M.; Chiarelli, R.; Rassat, A. *Angew. Chem., Int. Ed. Engl.* **1992**, *31*, 180−181.

(16) (a) Mileo, E.; Yi, S.; Bhattacharya, P.; Kaifer, A. E. *Angew. Chem., Int. Ed.* **2009**, *48*, 5337−5340. (b) Bardelang, D.; Banaszak, K.; Karoui, H.; Rockenbauer, A.; Waite, M.; Udachin, K.; Ripmeester, J. A.; Ratcliffe, C. I.; Ouari, O.; Tordo, P. *J. Am. Chem. Soc.* **2009**, *131*, 5402−5404. (c) Bardelang, D.; Rockenbauer, A.; Finet, J.-P.; Karoui, H.; Tordo, P. *J. Phys. Chem. B* **2005**, *109*, 10521−10530.

(17) (a) Hardy, M.; Bardelang, D.; Karoui, H.; Rockenbauer, A.; Finet, J.-P.; Jicsinszky, L.; Rosas, R.; Ouari, O.; Tordo, P. *Chem.—Eur. J.* **2009**, *15*, 11114−11118. (b) Vasquez-Vivar, J.; Kalyanaraman, B.; Martasek, P.; Hogg, N.; Masters, B. S. S.; Karoui, H.; Tordo, P.; Pritchard, K. A., Jr. *Proc. Natl. Acad. Sci. U.S.A.* **1998**, *95*, 9220−9225.

(18) (a) Tebben, L.; Studer, A. *Angew. Chem., Int. Ed.* **2011**, *50*, 5034−5068. (b) Clément, B.; Trimaille, T.; Alluin, O.; Gigmes, D.; Mabrouk, K.; Féron, F.; Decherchi, P.; Marqueste, T.; Bertin, D. *Biomacromolecules* **2009**, *10*, 1436−1445.

(19) (a) Hicks, R. G., Ed. *Stable Radicals: Fundamentals and Applied Aspects of Odd-Electron Compounds*; John Wiley & Sons: Chichester, U.K., 2010. (b) Kao, J. P.; Barth, E. D.; Burks, S. R.; Smithback, P.; Mailer, C.; Ahn, K. H.; Halpern, H. J.; Rosen, G. M. *Magn. Reson. Med.* **2007**, *58*, 850−854. (c) Hyodo, F.; Matsumoto, K.; Matsumoto, A.; Mitchell, J. B.; Krishna, M. C. *Cancer Res.* **2006**, *66*, 9921−9928. (d) Li, H.; He, G.; Deng, Y.; Kuppusamy, P.; Zweier, J. L. *Magn. Reson. Med.* **2006**, *55*, 669−675.

(20) (a) Rossini, A. J.; Zagdoun, A.; Lelli, M.; Canivet, J.; Aguado, S.; Ouari, O.; Tordo, P.; Rosay, M.; Maas, W. E.; Copéret, C.; Farrusseng, D.; Emsley, L.; Lesage, A. *Angew. Chem., Int. Ed.* **2012**, *51*, 123−127. (b) Zagdoun, A.; Rossini, A. J.; Gajan, D.; Bourdolle, A.; Ouari, O.; Rosay, M.; Maas, W. E.; Tordo, P.; Lelli, M.; Emsley, L.; Lesage, A.; Copéret, C. *Chem. Commun.* **2012**, *48*, 654−656. (c) Salnikov, E.; Rosay, M.; Pawsey, S.; Ouari, O.; Tordo, P.; Bechinger, B. *J. Am. Chem. Soc.* **2010**, *132*, 5940−5941. (d) Matsuki, Y.; Maly, T.; Ouari, O.; Karoui, H.; Le Moigne, F.; Rizzato, E.; Lyubenova, S.; Herzfeld, J.; Prisner, T.; Tordo, P.; Griffin, R. G. *Angew. Chem., Int. Ed.* **2009**, *48*, 4996−5000.

(21) Bardelang, D.; Giorgi, M.; Hornebecq, V.; Stepanov, A.; Rizzato, E.; Zaman, Md. B.; Chan, G.; Ouari, O.; Tordo, P. *RSC Adv.* **2012**, *2*, 5605−5609.

(22) Bardelang, D.; Giorgi, M.; Pardanaud, C.; Hornebecq, V.; Rizzato, E.; Tordo, P.; Ouari, O. *Chem. Commun.* **2013**, *49*, 3519−3521.

(23) Udachin, K. A.; Ratcliffe, C. I.; Enright, G. D.; Ripmeester, J. A. *Angew. Chem., Int. Ed.* **2008**, *47*, 9704−9707.

(24) (a) Castellano, R. K. *Curr. Org. Chem.* **2004**, *8*, 845−865. (b) Steiner, T. *Angew. Chem., Int. Ed.* **2002**, *41*, 48−76. (c) Desiraju, G. R. *Acc. Chem. Res.* **2002**, *35*, 565−573. (d) Taylor, R.; Kennard, O. *J. Am. Chem. Soc.* **1982**, *104*, 5063−5070.

(25) (a) Desiraju, G. R. *Acc. Chem. Res.* **1996**, *29*, 441−449. (b) Desiraju, G. R. *Acc. Chem. Res.* **1991**, *24*, 290−296.

(26) A Hirshfeld surface wrapping a molecule represents its contact boundaries related to closely packed surrounding molecules such that they never overlap. The d_{norm} parameter that can be mapped on it represents a contact distance of atoms of the considered molecule (inner to the Hirshfeld surface) with respect to the ones of neighboring molecules in the crystal (outer to the Hirshfeld surface). It is usually pictured such that red, white, and blue areas denote inner surface atoms that are at a distance, respectively, shorter than, almost equal to, and longer than the sum of van der Waals radii with respect to the closest atoms of surrounding molecules. For an introduction to Hirshfeld surfaces, graphical tools, and relevant examples: (a) Spackman, M. A.; Byrom, P. G. *Chem. Phys. Lett.* **1997**, *267*, 215−220. (b) Spackman, M. A.; McKinnon, J. J. *CrystEngComm* **2002**, *4*, 378−392. (c) McKinnon, J. J.; Spackman, M. A.; Mitchell, A. S. *Acta Crystallogr., Sect. B* **2004**, *60*, 627−668. (d) Spackman, M. A.; Jayatilaka, D. *CrystEngComm* **2009**, *11*, 19−32.

(27) Wolff, S. K.; Grimwood, D. J.; McKinnon, J. J.; Jayatilaka, D.; Spackman, M. A. *CrystalExplorer2.1*; University of Western Australia: Crawley, Western Australia, 2007. http://hirshfeldsurface.net/CrystalExplorer.

(28) Rozantsev, E. G.; Gur'yanova, E. N. *Russ. Chem. Bull.* **1966**, *15*, 936−939.

(29) Ysacco, C.; Rizzato, E.; Virolleaud, M. A.; Karoui, H.; Rockenbauer, A.; LeMoigne, F.; Siri, D.; Ouari, O.; Griffin, R. G.; Tordo, P. *Phys. Chem. Chem. Phys.* **2010**, *12*, 5841−5845.

(30) Ysacco, C.; Karoui, H.; Casano, G.; Le Moigne, F.; Combes, S.; Rockenbauer, A.; Rosay, M.; Maas, W.; Ouari, O.; Tordo, P. *Appl. Magn. Reson.* **2012**, *43*, 251−261.

(31) Dane, E. L.; Corzilius, B.; Rizzato, E.; Stocker, P.; Maly, T.; Smith, A. A.; Griffin, R. G.; Ouari, O.; Tordo, P.; Swager, T. M. *J. Org. Chem.* **2012**, *77*, 1789−1797.

(32) Rosen, G. M.; Schneider, E.; Shortkroff, S.; Tsai, P.; Winalski, C. S. *J. Chem. Soc., Perkin Trans. 1* **2002**, *23*, 2663−2667.

(33) For X-ray data of the corresponding dense phase, see the Supporting Information.

(34) (a) MacDonald, J. C.; Whitesides, G. M. *Chem. Rev.* **1994**, *94*, 2383−2420. (b) Philp, D.; Stoddart, J. F. *Angew. Chem., Int. Ed. Engl.* **1996**, *35*, 1154−1196. (c) Lehn, J.-M. *Chem.—Eur. J.* **2000**, *6*, 2097−2102. (d) Whitesides, G. M.; Grzybowski, B. *Science* **2002**, *295*, 2418−2421.

(35) (a) Lim, S.; Kim, H.; Selvapalam, N.; Kim, K.-J.; Cho, S. J.; Seo, G.; Kim, K. *Angew. Chem., Int. Ed.* **2008**, *47*, 3352−3355. (b) Msayib, K. J.; Book, D.; Budd, P. M.; Chaukura, N.; Harris, K. D. M.; Helliwell, M.; Tedds, S.; Walton, A.; Warren, J. E.; Xu, M.; McKeown, N. B. *Angew. Chem., Int. Ed.* **2009**, *48*, 3273−3277. (c) Dalrymple, S. A.; Shimizu, G. K. H. *J. Am. Chem. Soc.* **2007**, *129*, 12114−12116. (d) Saied, O.; Maris, T.; Wang, X.; Simard, M.; Wuest, J. D. *J. Am. Chem. Soc.* **2005**, *127*, 10008−10009. (e) Brunet, P.; Simard, M.; Wuest, J. D. *J. Am. Chem. Soc.* **1997**, *119*, 2737−2738.

(36) (a) Ananchenko, G. S.; Moudrakovski, I. L.; Coleman, A. W.; Ripmeester, J. A. *Angew. Chem., Int. Ed.* **2008**, *47*, 5616−5618. (b) Brouwer, E. B.; Enright, G. D.; Udachin, K. A.; Lang, S.; Ooms, K. J.; Halchuk, P. A.; Ripmeester, J. A. *Chem. Commun.* **2003**, *12*, 1416−

1417. (c) Atwood, J. L.; Barbour, L. J.; Jerga, A.; Schottel, B. L. *Science* **2002**, *298*, 1000−1002.
(37) (a) Süss, H. I.; Lutz, M.; Hulliger, J. *CrystEngComm* **2002**, *4*, 610−612. (b) Makha, M.; McKinnon, J. J.; Sobolev, A. N.; Spackman, M. A.; Raston, C. L. *Chem.—Eur. J.* **2007**, *13*, 3907−3912. (c) Makha, M.; Scott, J. L.; Strauss, C. R.; Sobolev, A. N.; Raston, C. L. *Cryst. Growth Des.* **2009**, *9*, 483−487. (d) Konarev, D. V.; Khasanov, S. S.; Otsuka, A.; Maesato, M.; Saito, G.; Lyubovskaya, R. N. *Angew. Chem., Int. Ed.* **2010**, *49*, 4829−4832. (e) Kobayashi, J.; Domoto, Y.; Kawashima, T. *Chem. Commun.* **2009**, *41*, 6186−6188.
(38) Gafurov, M.; Lyubenova, S.; Denysenkov, V.; Ouari, O.; Karoui, H.; Le Moigne, F.; Tordo, P.; Prisner, T. *Appl. Magn. Reson.* **2009**, *37*, 505−514.
(39) (a) Hanson, G. R.; Jensen, P.; McMurtrie, J.; Rintoul, L.; Micallef, A. S. *Chem.—Eur. J.* **2009**, *15*, 4156−4164. (b) Mugnaini, V.; Punta, C.; Liantonio, R.; Metrangolo, P.; Recupero, F.; Resnati, G.; Pedulli, G. F.; Lucarini, M. *Tetrahedron Lett.* **2006**, *47*, 3265−3269.
(40) (a) Laliberte, D.; Maris, T.; Wuest, J. D. *J. Org. Chem.* **2004**, *69*, 1776−1787. (b) Sauriat-Dorizon, H.; Maris, T.; Wuest, J. D. *J. Org. Chem.* **2003**, *68*, 240−246.
(41) (a) Potts, S. V.; Barbour, L. J.; Haynes, D. A.; Rawson, J. M.; Lloyd, G. O. *J. Am. Chem. Soc.* **2011**, *133*, 12948−12951. (b) Soegiarto, A. C.; Yan, W.; Kent, A. D.; Ward, M. D. *J. Mater. Chem.* **2011**, *21*, 2204−2219. (c) Kobayashi, H.; Ueda, T.; Miyakubo, K.; Eguchi, T.; Tani, A. *Bull. Chem. Soc. Jpn.* **2007**, *80*, 711−720. (d) Kobayashi, H.; Ueda, T.; Miyakubo, K.; Toyoda, J.; Eguchi, T.; Tani, A. *J. Mater. Chem.* **2005**, *15*, 872−879. (e) Süss, H. I.; Wuest, T.; Sieber, A.; Althaus, R.; Budde, F.; Lüthi, H.-P.; McManus, G. D.; Rawson, J.; Hulliger, J. *CrystEngComm* **2002**, *4*, 432−439. (f) Langley, P. J.; Rawson, J. M.; Smith, J. N. B.; Schuler, M.; Bachmann, R.; Schweiger, A.; Palacio, F.; Antorrena, G.; Gescheidt, G.; Quintel, A.; Rechsteiner, P.; Hulliger, J. *J. Mater. Chem.* **1999**, *9*, 1431−1434.
(42) (a) Inokuma, Y.; Kawano, M.; Fujita, M. *Nat. Chem.* **2010**, *3*, 349−358. (b) Hurd, J. A.; Vaidhyanathan, R.; Thangadurai, V.; Ratcliffe, C. I.; Moudrakovski, I. L.; Shimizu, G. K. H. *Nat. Chem.* **2009**, *1*, 705−710.